



LAWRENCE  
LIVERMORE  
NATIONAL  
LABORATORY

# Value of Information Evaluation using Field Data

W. Trainor-Guitton

December 10, 2014

## **Disclaimer**

---

This document was prepared as an account of work sponsored by an agency of the United States government. Neither the United States government nor Lawrence Livermore National Security, LLC, nor any of their employees makes any warranty, expressed or implied, or assumes any legal liability or responsibility for the accuracy, completeness, or usefulness of any information, apparatus, product, or process disclosed, or represents that its use would not infringe privately owned rights. Reference herein to any specific commercial product, process, or service by trade name, trademark, manufacturer, or otherwise does not necessarily constitute or imply its endorsement, recommendation, or favoring by the United States government or Lawrence Livermore National Security, LLC. The views and opinions of authors expressed herein do not necessarily state or reflect those of the United States government or Lawrence Livermore National Security, LLC, and shall not be used for advertising or product endorsement purposes.

This work performed under the auspices of the U.S. Department of Energy by Lawrence Livermore National Laboratory under Contract DE-AC52-07NA27344.

## Table of Contents

<b>Section 1. Introduction</b> .....	<b>4</b>
Objective, impact, and summary .....	4
Work accomplished this year .....	4
<b>Section 2. Milestones and progress</b> .....	<b>6</b>
<b>Section 3. References</b> .....	<b>8</b>
<b>Appendix A. World Geothermal Congress Paper</b> .....	<b>9</b>
<b>Appendix B. Additional publications (as separate documents)</b> .....	<b>31</b>

# *Section 1*

---

## *Introduction*

---

### **Objective, impact, and summary**

Value of information (VOI) provides the ability to distinguish between useful and frivolous information gathering for a geothermal prospect, either hydrothermal or for enhanced geothermal systems. Useful information provides a value greater than the cost of the information; wasteful information costs more than the expected value of the information. In this project we applied and refined VOI methodologies on selected geothermal prospects. This will directly contribute to GTP priorities by:

- decreasing drilling cost by assessing the development risk with and without additional information.
- advancing subsurface imaging capabilities by providing a workflow for determining the “worth” of geophysical data in context of the production decision.

The goal of the project was to develop and document a value of information workflow that utilizes real field data from a geothermal field. The objective was to use calibrated field data in order to compare the exploration information (i.e. surface geophysics, well logging data, etc.) to the drilling or production results (flow, temperature, etc). The data analyzed uses data provided in-kind by an industry partner (Chevron) in an existing geothermal field. The result an estimation of whether a particular set of information is worth acquiring or purchasing.

The methodology was designed so that operators can apply the workflow to establish which types of data should be collected for a new field. This will be based on the past performance of the information in determining geothermal parameters that control the economic potential of a geothermal reservoir. Previous work (Trainor-Guitton et al., 2014; 2013a,b) demonstrated the use of synthetic datasets to estimate the reliability of the VOI estimate. Here, this work is extended to real data sets from an operating geothermal production field.

### **Work accomplished this year**

As mentioned above, the goals of the current work are to conduct a VOI study on a real geothermal dataset. The dataset is from the from the Darajat geothermal field in Indonesia. Darajat is a vapor-dominated volcanic reservoir in West Java that generates approximately 260 Mw from three power plants (Rejeki et al., 2012). The underlying geology consists mainly of

pyroclastics and lavas, with permeability controlled largely by lithology. Geophysical surveys included a magneto-telluric (MT) survey that allowed construction of a conductivity model. The goal is to determine how well electrical conductivity is useful as a predictor of well stream flow rates using VOI.

The work was broken down into a set of four milestones:

**Q1:** Dataset will be in hand and preliminary statistical analysis performed (calibration) on available variables. COMPLETE.

**Q2:** Preliminary VOI result using statistics of one calibrated dataset (e.g. the value of MT (conceivably in monetary units) given the reliability measure from field data and a few different prior uncertainty measures). COMPLETE.

**Q3:** Refinement of VOI results using statistics of calibrated dataset; possible additional variables added (e.g. remove previous assumptions, improve previous analysis and/or provide further analysis such as spatial uncertainty). COMPLETE.

**Q4:** Final VOI result using statistics of dataset. The value of MT (and perhaps other techniques) will be provided, along with a workflow of how this transfers to other datasets. 85% COMPLETE.

Progress was good, although progress on the third and fourth milestones was delayed. The progress on each milestone will be detailed in the next section. Several publications were made or completed during the time period. These are included or attached to this report.

Whitney J. Trainor-Guitton, G. Michael Hoversten, Gregg Nordquist, Rindu Grahabhakti Intani, Robert Mellors, and Jeffery Roberts, 2015, Value of MT inversions for geothermal exploration: accounting for multiple interpretations of field data & determining new drilling locations, originally submitted and accepted to the World Geothermal Congress, accepted, and now withdrawn.

Trainor-Guitton, W. J., G. M. Hoversten, A. Ramirez, J. Roberts, E. Juliusson, K. Key, and R. Mellors, 2014a, The value of spatial information of for determining well placement: a geothermal example, *GEOPHYSICS* 79, 5(2014); pp. W27-W41 (15 pages)  
<http://dx.doi.org/10.1190/geo2013-0337.1>, Online Publication Date: 25 Aug 2014

Trainor-Guitton, W., M. Hoversten, E. Juliusson, A. Ramirez, J. Roberts, and R. Mellors, 2014b, Value of Information Assessment using Calibrated Geothermal Field Data, Proceedings of the 39th Stanford Geothermal Workshop, Feb. 24-26, 2014, Stanford, CA.

## *Section 2*

---

### *Milestones and progress*

---

#### **Q1 Milestone: Dataset will be in hand and preliminary statistical analysis performed (calibration) on available variables.**

The goal is to determine how well electrical conductivity can determine possible steam flow rates and to make this assessment with real field data. In October 2013, Chevron provided 3D electrical conductivity model and 23 steam flow measurements from the Darajat geothermal field in Indonesia. The 3D conductivity model derives from a 3D inversion of MT survey data from the Darajat field.

EarthVision tools were used to define several possible interpretations of the clay cap, which is indicative of geothermal alteration and used to determine locations for drilling. Initially, contours of the steam flow data were also generated using EarthVision to extrapolate steam flow measurements. In a separate Python code, comparisons were made between steam flow measurements and “co-located” electrical conductivity: conductivities that are within the clay cap that were deemed within a search radius of 650m.

#### **Q2 Milestone: Preliminary VOI result using statistics of one calibrated dataset (e.g. the value of MT (conceivably in monetary units) given the reliability measure from field data and a few different prior uncertainty measures).**

Several modifications were made to the calibration definition after several teleconferences with Chevron. First, it was decided to use the raw steam flow measurements rather than the contoured values. Second, the conductance (the product of conductivity and thickness of the clay cap) is expected to better correlate with steam flow than conductivity alone, as the thickness of the clay cap is expected to thin with higher temperatures. These modifications, along with a preliminary VOI results, were presented at the Stanford Geothermal Workshop in February 2014.

#### **Q3 Milestone: Refinement of VOI results using statistics of calibrated dataset; possible additional variables added (e.g. remove previous assumptions, improve previous analysis and/or provide further analysis such as spatial uncertainty).**

Several enhancements were made in this quarter. These were incorporated in a submitted and accepted World Geothermal Congress paper (see Appendix). Several prior uncertainties were incorporated to achieve different VOI results given different perceive initial risks.

A comparison of clay cap models, based on two different methods, was conducted. One model was defined using gridded and contoured 1D MT inversion models. The other model used the 3D inversion model. The resulting VOI for each model differed but not significantly from the perspective of decision analysis as the different VOI's were within \$4,000 of each other, and therefore, the decision to purchase MT or not would be the same given the result of these VOI's.

A spatial analysis was performed by using the calibration to determine future drilling locations in Darajat. The calibration is a probabilistic relationship between electrical conductance and steam flow. This was used to identify locations within the Darajat field that have the highest probability of success, given conductance's past performance to predict steam flow. The value metric was then mapped back onto the conductance field of the Darajat geothermal field.

**Q4 Milestone: Final VOI result using statistics of dataset. The value of MT (and perhaps other techniques) will be provided, along with a workflow of how this transfers to other datasets.**

After examining the results of the mapping of the value metric on the geothermal field, it was realized that the results could be further improved by a different treatment of conductance's that are not represented in the original calibration set. Certain ranges of conductance's are not classified as "co-located" to steam flow measurements, thus they are "missing" in the calibration set (the subset of data that determines the relationship between conductance and steam flow). In the VOI analysis, these conductance's are given equal probability of relating to all the steam flow classifications, which is a fair or conservative method for handling them. However, when VOI maps were made, this approach led to low values being assigned where there is known high steam flow production. Therefore, some type of extrapolation methods are required in handling these conductance values that aren't represented in the calibration set. This revision has not yet been completed. It was decided not to present the work until the revised higher-resolution process is complete. Therefore, the WGC paper, which used the low-resolution analysis, will be withdrawn, but it is intended to present at Geothermal Resource Council 2015 or Stanford Geothermal Workshop 2016.

We consider that this milestone is 90% complete, since sensible VOI methodology and subsequent VOI metrics have been produced. However, this problem of "missing" data is a result of using real field data, and it will be important and useful to demonstrate better ways of handling it for future applications.

## Section 3

---

### References

---

- Rejeki, S., D. Rohrs, G. Nordquist, and A. Fitriyanto**, 2010. Geologic Conceptual Model Update of the Darajat Geothermal Field , Indonesia. In *Proceedings World Geothermal Congress 2010* (pp. 25–29).
- Trainor-Guitton, W. J., G. M. Hoversten, G. Nordquist, R. G. Intani, R. Mellors, and J. Roberts**, 2015, Value of MT inversions for geothermal exploration: accounting for multiple interpretations of field data & determining new drilling locations, submitted to the World Geothermal Congress,
- Trainor-Guitton, W. J., G. M. Hoversten, A. Ramirez, J. Roberts, E. Juliusson, K. Key, and R. Mellors**, 2014a, The value of spatial information of for determining well placement: a geothermal example, *GEOPHYSICS* 79, 5(2014); pp. W27-W41 (15 pages)  
<http://dx.doi.org/10.1190/geo2013-0337.1>, Online Publication Date: 25 Aug 2014
- Trainor-Guitton, W., M. Hoversten, E. Juliusson, A. Ramirez, J. Roberts, and R. Mellors**, 2014b, Value of Information Assessment using Calibrated Geothermal Field Data, Proceedings of the 39th Stanford Geothermal Workshop, Feb. 24-26, 2014, Stanford, CA.
- Trainor-Guitton, W., A. Ramirez, J. Ziagos, R. Mellors and J. Roberts**, 2013a, An Initial Value of Information (VOI) Framework for Geophysical Data Applied to the Exploration of Geothermal Energy, Proceedings of the 38<sup>th</sup> Stanford Geothermal Workshop, Feb. 11-13, 2013, Stanford, CA.
- Trainor-Guitton, W. J., A. Ramirez, J. Ziagos, R. Mellors, J. Roberts, E. Juliusson, and M. G. Hoversten**, 2013b, Value of Spatial Information for Determining Geothermal Well Placement, *Geothermal Resources Council Transaction*

# *Appendix A*

## *World Geothermal Congress Paper*

### **Value of MT inversions for geothermal exploration: accounting for multiple interpretations of field data & determining new drilling locations**

Whitney J. Trainor-Guitton<sup>1</sup>, G. Michael Hoversten<sup>2</sup>, Gregg Nordquist<sup>3</sup>, Rindu Grahabhakti Intani<sup>4</sup>, Robert Mellors<sup>1</sup>, and Jeffery Roberts<sup>1</sup>

<sup>1</sup>Lawrence Livermore National Laboratory, 7000 East Avenue  
trainorguitton@llnl.gov

<sup>2</sup>Chevron Energy Technology Company, San Ramon, CA

<sup>3</sup>Chevron Geothermal Services Company, Makati City, Philippines

<sup>4</sup>Chevron Geothermal Power Indonesia, Jakarta, Indonesia

**Keywords:** value of information, resource assessment, magnetotellurics

#### **Abstract**

How well does geophysical data improve our geothermal prospecting decisions? How much is this information worth? These types of questions can be answered using the value of information (VOI) method. VOI quantifies how relevant any particular information source is, given a decision with an uncertain outcome; thus, the estimated VOI can be used to justify the purchase of additional data when exploring for geothermal resources. Previously, a value of information (VOI) methodology using synthetic data for the exploration geothermal problem was presented (Trainor-Guitton et al., 2014). Evaluating the reliability of a geophysical method to decipher key spatial subsurface features is relatively straightforward with synthetic data since many different “true” subsurface models can be tested.

Perhaps a more useful analysis is to decipher the reliability of field data that has been “calibrated,” e.g. production parameters have been observed that are approximately collocated with the geophysical data. Specifically, we consider a 3D electrical resistivity model that has been constructed from MT (magnetotellurics) data via geophysical inversion. We are especially interested in how multiple interpretations of the inversion model can be incorporated into the reliability analysis. Typically, MT data are used to detect the electrically conductive clay cap which can be indicative of geothermal alteration occurring just above the resource. Several interpretations of the clay cap (a 3D feature) are possible and may result in different estimates of the effectiveness of the MT technique to detect electrically conductive targets that can be indicative of potential geothermal resources, representative of the well data (steam flow,

permeability and pressure). We will present several alternative interpretations that will highlight the challenges and advantages of using field data to estimate the value of geophysical information. Our results, however, indicate that the final VOI estimate was not strongly dependent on the different interpretations of the MT data set. Additionally, we demonstrate how these VOI evaluations can be used to guide future drilling locations.

## 1. Introduction

The value of information (VOI) quantifies how relevant and reliable any particular information source is, and quantifies its value when making a decision with an uncertain outcome. VOI can be used to justify the costs of collecting and processing the planned data. It has been used in oil exploration (see review by Bratvold et al., 2009). We apply it here to geophysical data from a geothermal field. Previous work (Trainor-Guitton et al., 2013a,b) tested the applicability for geothermal exploration using synthetic datasets.

VOI is a method from the field of decision analysis. Decision analysis concepts are often described in terms of lotteries and prizes (Pratt et al., 1995). By choosing to drill or not, a decision maker is choosing whether or not to participate in a lottery with certain perceived chances of winning a prize (drilling into a profitable reservoir); however, this lottery also involves the chances of losing money (drilling into an uneconomic reservoir). VOI estimates the possible increase in expected utility (winning a lottery with a bigger prize) by gathering information before making a decision, such as where or if to drill a production well. In its simplest form, the VOI equation can be expressed as:

$$VOI = V_{with\ information} - V_{prior} \quad (1)$$

where V is the value, the metric used to quantify the outcome of a decision. The higher the value, the more “successful” an outcome of a decision is. Therefore, value is the revenue gained minus the costs incurred for any particular decision action taken. The simplest representation of the decision in geothermal exploration is “to drill or not” for one particular location; if heat, permeability and fluids exist in that location, then the value outcome of that decision will be high. Otherwise, the value outcome will be a monetary loss.

We consider how well the clay cap, as delineated by a 3D MT data inversion, can indicate magnitude of the steam flow by utilizing a dataset from an operating geothermal field. The electrically conductive materials imaged by MT are created by geochemical alteration when hot fluids circulate within subsurface geologic units (Gunderson et al., 2000). However, if the hot fluid source ceases to exist, the electrically conductive material will remain, thus a clay cap does not guarantee current geothermal activity (Karlisdóttir et al., 2012).

The contributions presented in this paper are twofold. First, our work illustrates the implementation of a VOI methodology given the uncertainties of geothermal exploration and multiple interpretations of the clay cap from a 3D MT inversion. We utilize an existing dataset of steam flow measurements to deduce trends between steam flow and electrical conductivity, thereby using the past performance of the geophysical technique to predict steam flow. The VOI’s produced can be used to determine if MT should be collected again in a field with similar geological and geophysical attributes. The second set of results presented here demonstrate how the VOI evaluations can serve as a guide on deciding where to drill for new production wells in undeveloped areas given that the MT information has already been collected in that area.

The paper is organized as follows. First the steam flow and MT data sets are described. Then we describe how the 3D cube of electrical conductivity is used to infer the location and margins of

the clay cap: the potential margins or boundaries of the geothermal reservoir. Third, we will describe the different set of assumptions used to determine three different clay caps and the colocation between the electrical conductivity of the clay cap and a steam flow measurement. The various conductivity and spatial thresholds produce various interpretations of the “calibrated dataset.” Fourth, these multiple interpretations will provide three estimates of the MT’s reliability to delineate the boundaries of the geothermal reservoir. Finally, we will use these reliabilities to 1) calculate VOI’s (values of information) of MT and 2) provide guidance on where future drilling should be focused.

### 1.1 Darajat geothermal field

Darajat is vapor geothermal field located in West Java, Indonesia. It is located about 150 km to the southeast of Jakarta and has an elevation ranging from 1,750 to 2,000 meters above sea level. First production from the field was started in 1994 with installation of a 55 MW plant. Additional capacity was added in 2000 and 2007 to bring the total production capacity to 271 MW from three power plants.

The Darajat geothermal field is located along a range of Quaternary volcanic centers in West Java. It is spatially associated with an eroded andesitic stratovolcano, Gunung Kendang. The reservoir is dominantly comprised of thick lava flows and intrusions in a stratovolcano central facies, with relatively higher porosity, thick pyroclastic sequences of proximal to medial facies that were deposited more toward the margins. Structures trend predominantly NE-SW but also include N-S and NW-SE trending faults (Rejeki et al., 2010).

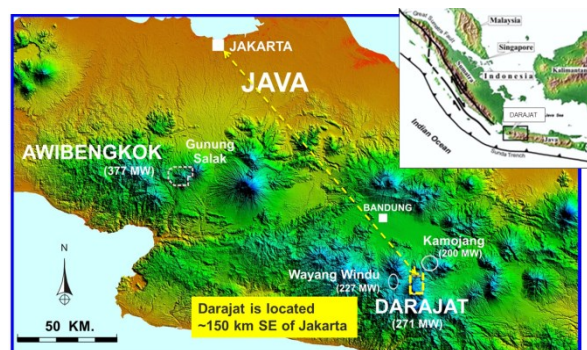


Figure 1: Location of the Darajat geothermal field in West Java

## 1.2 Data sets used in this study

### 1.2.1 Steam flow measurements

The steam flow dataset contains the average production over one year for 23 different wells. The steam flow data approximately spans an area of 2.6 km by 4.2 km and a depth range of 600m to 1800m below the surface. Figure 2 displays a histogram of these steam flow measurements. The steam flow measurements are composite flows for all feed zones from each well.

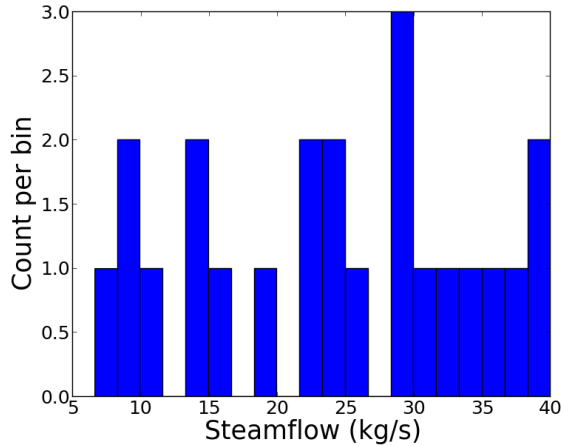


Figure 2: Histogram of steam flow data from 23 wells.

For this VOI demonstration, we categorized the *steam flow magnitude* into seven groups or bins, represented by  $\theta_i$ :

$$\theta_i \ i \in \begin{cases} 7, & \theta \geq 30 \text{ kg/s} \\ 6, & 25 \leq \theta < 30 \text{ kg/s} \\ 5, & 20 \leq \theta < 25 \text{ kg/s} \\ 4, & 15 \leq \theta < 20 \text{ kg/s} \\ 3, & 10 \leq \theta < 15 \text{ kg/s} \\ 2, & 5 \leq \theta < 10 \text{ kg/s} \\ 1, & 0 \leq \theta < 5 \text{ kg/s} \end{cases} \quad (2)$$

We define our prior uncertainty with respect to steam flow production using these steam flow categories. Let us represent this by

$$\mathbf{z}(\theta_i) \quad i = 1, \dots, 7, \quad (3)$$

where vector  $\mathbf{z}$  represents the non-dimensional steam flow categories that may be realized from production wells. Future work could incorporate spatial aspects of this steam flow possibility. The steam flow categories can be used to represent the economic (value) outcome of a drilling decision at any location  $(x, y, z)$ .

Figure 2 reveals that the steam flow data does not include any measurements  $< 5$  kg/s. This is understandable since the wells are drilled with the intention of placing them where steam flow will be high. This bias in the data, however, will pose challenges in assigning what conductance's are representative of this steam flow category, described in Section 2.3. Table 1 summarizes the probability of occurrence for each of the steam flow categories ( $Pr(\theta = \theta_i)$ ) according to the data (a) and three other hypothetical prior probabilities (b-d) that will be used later for the value of information analysis. These probabilities should be derived from expert opinion and all other data available for the particular site. The priors in columns b-d are chosen for demonstration purposes and are not related to the Darajat field per se.

**Table 1: Prior probabilities of steam flow categories according to the data and other projections**

↓Steam Flow Rate (kg/s)	a) Percentage of steam flow data in each category	b) Least optimistic $Pr(\Theta = \theta_i)$	c) Intermediate $Pr(\Theta = \theta_i)$	d) Most optimistic $Pr(\Theta = \theta_i)$
$\theta_i > 30$	30.4%	10%	13%	40%
$25 \leq \theta_i \leq 30$	17.4%	10%	13%	10%
$20 \leq \theta_i \leq 25$	17.4%	10%	13%	10%
$15 \leq \theta_i \leq 20$	8.7%	10%	13%	10%
$10 \leq \theta_i \leq 15$	13.0%	10%	13%	10%
$5 \leq \theta_i \leq 10$	13.0%	10%	15%	10%
$\theta_i \leq 5$	0%	40%	20%	10%

### 1.2.2 Magnetotellurics

The MT data used for this analysis consists of 85 remote referenced stations which were distributed over and outside the boundaries of the Darajat geothermal field. The data were collected in 1996-97 and 2004 and were used to interpret the distribution and extensions of the electrically conductive clay cap beyond the first development area (Rejeki et al., 2010). For the interpretation of the clay cap, two approaches were used. For the 3D inversion of the data set, the off-diagonal impedances between 100 seconds and 100 Hertz were inverted using the 3D algorithm of Newman and Alumbaugh (2000). The impedance errors derived from the multi-station robust processing were used subject to a 10% error floor. The starting model was a 10  $\Omega$ m half-space beneath the topography. The inversion reduced the RMS data misfit from 87 to 1.3. For the 1D approach for defining the clay cap, 1D inverted models using the Transverse Electric (TE) mode were used to define the resistivity and thickness of the conductive layer.

## 2. Methodology

Our methodology estimates the prediction power of MT given a collocated steam flow dataset. First, we consider the decision of “to drill or not,” and we make several evaluations of the efficacy of MT via several interpretations of the MT inversion model. It is possible to extend the methodology to the more complex decision of “where to drill.” We assume that the decision outcome only depends on the possible steam flow of a reservoir.

### 2.1 Interpretations of clay cap: different conductivity thresholds only

We have one 3D model of conductivity inverted from the MT dataset described above which overlies where the steam flow measurements were made. First, we use only this inversion model to determine possible relationships between the electrical conductivity property and the steam flow magnitude. Typically, the high conductivity layer can be used to estimate the likely margins of the geothermal system (Cumming, 2009). We attempt to assess whether the thickness and conductivity information of the clay cap can be used to distinguish between higher and lower steam flow.

As we assume that the “clay cap” margins can be used to infer the boundaries of the geothermal resource, we define a conductivity threshold in order to delineate the location and thickness of the clay cap. We use a bottom threshold value of  $\sigma=0.12$  S/m. Thus, a top and bottom surface is defined where the electrical conductivity begins to decrease from the threshold value of  $\sigma=0.12$  S/m. The resulting cap is pictured in Figure 3.

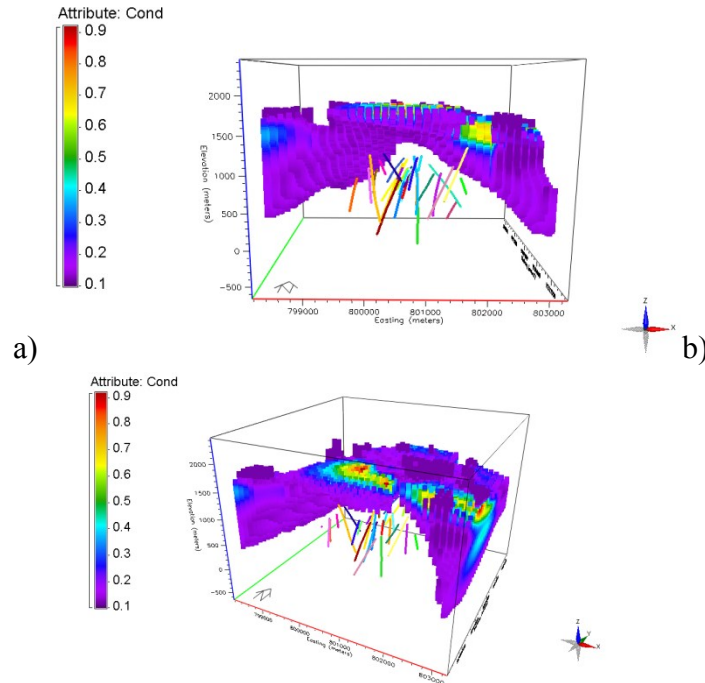


Figure 3: a) Cross sectional view and b) top view of clay, defined by threshold  $\sigma=0.12$  S/m. Wells containing steam flow measurements shown in multicolor.

### 2.1.1 Defining “collocated” electrical conductivity and steam flow

Next, we determine which conductivity locations within the clay cap that can be correlated with the steam flow measurements. We suggest that steam flow measurements closer to the cap are more likely to influence the electrical conductivities and geometry of the clay cap. Therefore, we expect a stronger relationship between the steam flow measurements that are closer to the clay cap.

We begin by defining 625m as the maximum distance between a steam flow measurement and any point within the clay cap. We choose this distance because it represents the lower quartile of all distances between the clay cap conductivities and steam flow locations. Figure 4a) displays the midpoint of the steam producing zone of Well 15 as a red box along the well path (red) and the conductivity values of the clay cap. First, the location of the closest conductivity measurement to the well midpoint is determined. Then, the neighboring conductivity values in the clay cap are averaged within a radius of 100 m to compare to the steam flow of that well. Figure 4b) displays only the conductivities measurements that are within 100m of the closest conductivity point for Well 15.

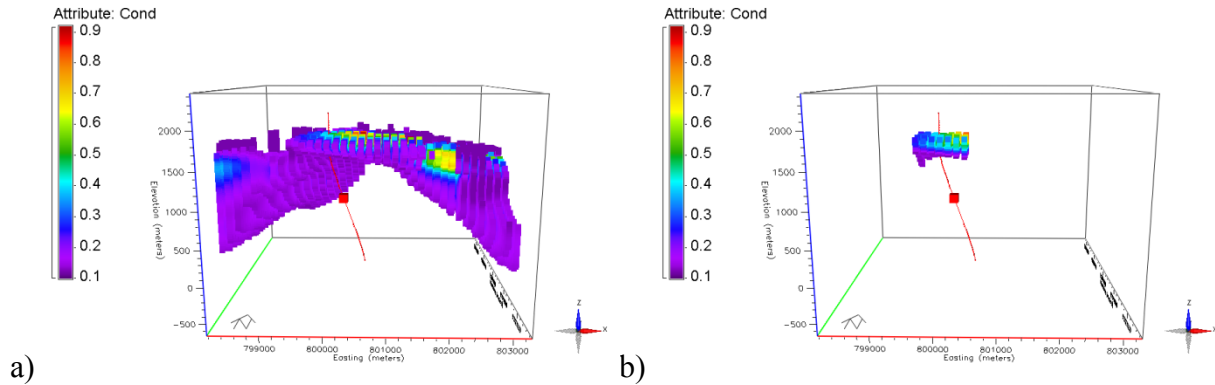


Figure 4: a) Well 15 midpoint (red box along red path) with conductivities of clay cap. b) Only the conductivities within 100m of the closest conductivity point to Well 15's midpoint.

This is repeated for any steam flow-clay cap pair that is less than 625m away. Figure 5a plots the geometric average of these neighboring conductivities versus the nearest steam flow measurement. Six of the 23 steam flow measurements locations were within the maximum threshold of 625m. Of this set, the conductivities show a slight positive correlation (0.36) with steam flow.

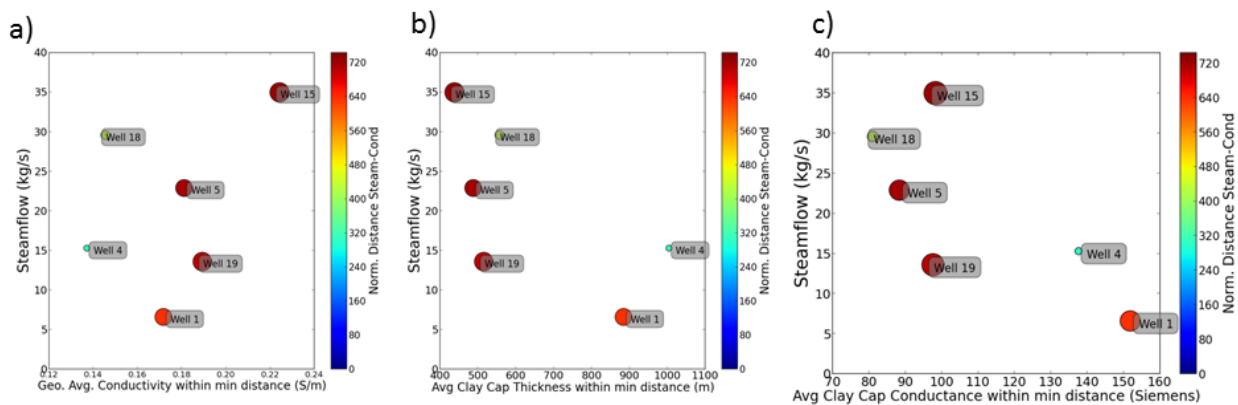


Figure 5: 2D scatterplot of co-located a) electrical conductivities (geometric average) b) thicknesses (arithmetic average) and c) conductance (all from 0.12S/m clay cap) and steam flow (maximum distance 625m). The size of the symbols reflects number of conductivities used in the average calculation and the color represents the distance

This same process is done for the clay cap thickness at these neighboring locations. Figure 5b displays the arithmetic average of the clay cap thickness versus the 6 steam flow measurements, and Figure 5c displays average conductance (the product of conductivity and clay cap thickness). Unlike Figure 5a, these two plots now show a relatively strong negative correlation with steam flow: -0.67 and -0.73 respectively. The negative correlation of steam flow with conductance (which is dominated by the thickness) is expected since greater temperatures (>200°C) will alter the highly conductive smectite clays into more resistive illitic or chloritic clays (Ussher et al., 2000). The clay cap for this analysis is defined on the basis of conductivity, and therefore it is expected to dominantly represent the distribution of smectite. Since places that have been altered to illite will have lower conductivity they tend not to be included in the clay cap interpretation as used in this analysis. Thus, if the interpreted clay cap based on the MT data is capturing only the higher conductive smectite, **one would expect a shallower base and a thinning of the clay cap over areas where the permeability is higher.** Therefore, we only consider and include the

conductance (not conductivity or thickness alone) for the next two interpretations of clay cap for comparison with the steam flow measurements.

Next, we tested how sensitive these results are to the threshold which defines the clay cap. We now define the clay cap with the threshold of 0.1 S/m. This clay cap, shown in Figure 6, is slightly thicker than the clay cap defined by the threshold of 0.12 S/m (Figure 3).

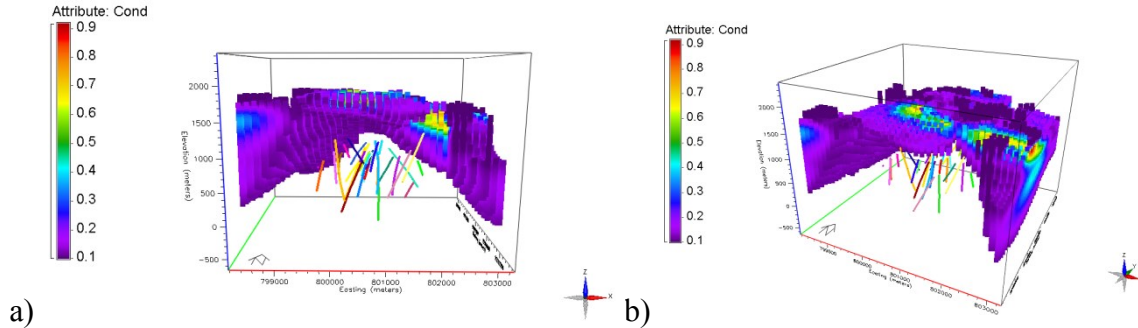


Figure 6: Cross sectional view of clay cap from the inversion that imposes fault boundaries defined by threshold  $\sigma=0.10$  S/m. Wells containing steam flow measurements shown in multicolor.

This thicker clay cap produces more pairs of steam flow/conductivity location pairs when using the maximum distance of 625m. Figure 7 only plots the eight steam flow measurements versus their neighboring conductance, since this relationship may be more revealing of reservoir temperature. The resulting correlation coefficient is -0.7.

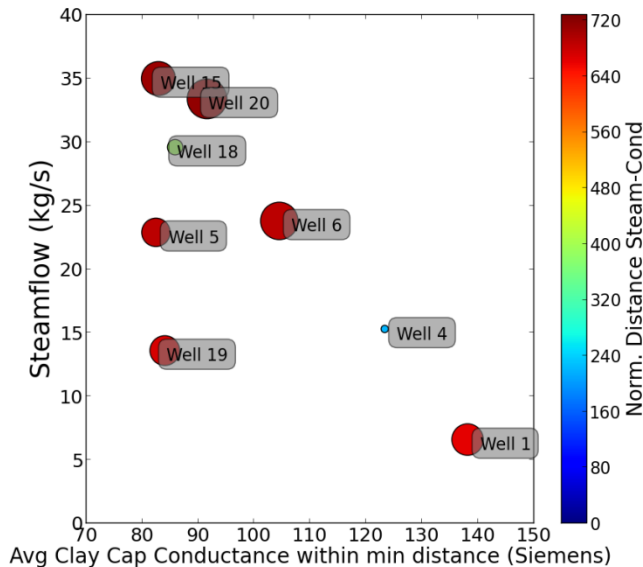


Figure 7: 2D scatterplot of co-located conductance (from 0.10S/m clay cap) and steam flow (maximum distance 625m). The size of the symbols reflects number of conductivities used to calculate the average and the color represents the distance

## 2.2 Integrated interpretation of clay cap

Another very commonly applied approach for interpretation of the clay cap is to use 1D models to define the conductive layer. In this case the distribution and characteristics of the conductive layer are interpreted from 1D interpretations of the TE mode. The characteristics of the conductive layer which include elevations of base and top, thickness and conductance for the layer are calculated for each MT station and then gridded and contoured to produce maps and

cross-section. These are then used by the interpreter interpret the clay cap and to extrapolate away from the wells. Figure 8 shows the interpretation of the top and base of the clay cap which was made using these data. This interpretation will tend to have a thicker cap than the defined conductivity cutoff value used in the 3D inversions above because it also contains higher resistivity parts of the cap.

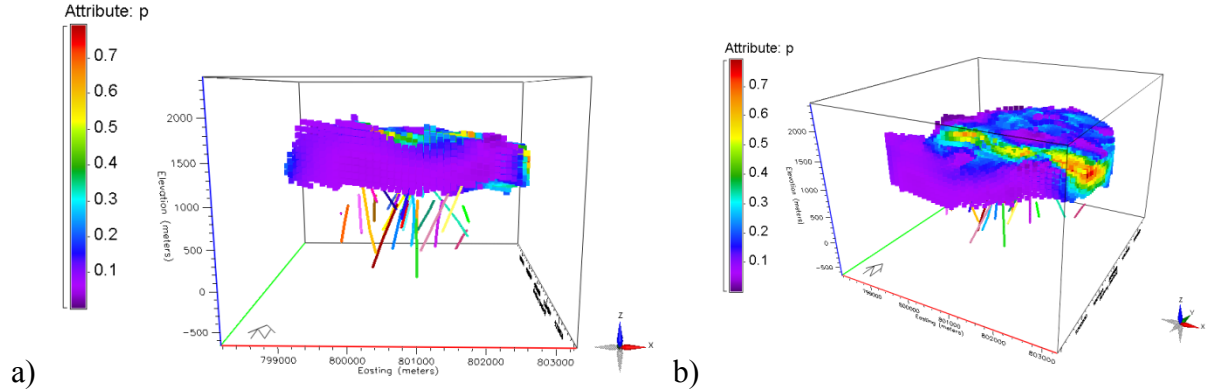


Figure 8: Clay cap defined by electrical conductivity, methylene blue analysis, and temperature isotherms

The clay cap base for this interpretation is much closer to steam flow measurements. The lower quartile of distances between the clay cap base and steam flow locations is ~500m, 125m less than clay cap base with electrical resistivity alone. Therefore, 20 wells were within 500m of the clay cap. Figure 9 contains the geometric averages of conductance versus the steam flow measurements (equivalent to Figure 7); the correlation coefficient is -0.53. The clay cap interpreted from the integrated analysis is thicker than the previous two (Figure 5c and Figure 7).

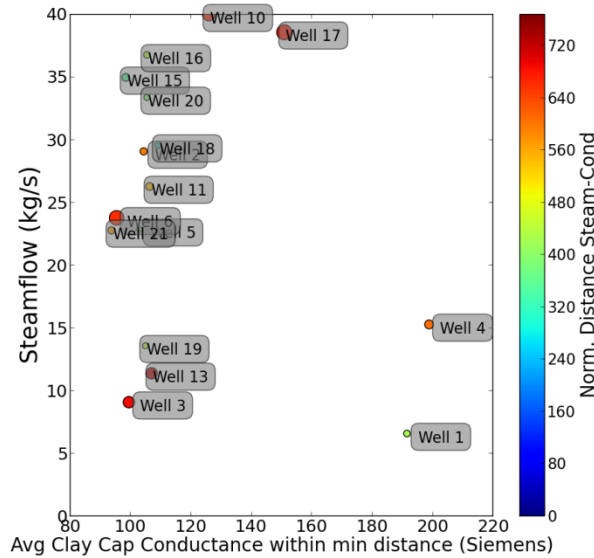


Figure 9: Averages of Conductance within 500m of steam flow measurements using the top and base of clay cap as determined by geology, methylene blue analysis and the MT inversion model

### 2.3 Establishing estimations of the data reliability/likelihood: How well does the conductance of the clay cap distinguish the steam flow categories?

As described in the Introduction, a data reliability or likelihood is necessary to evaluate VOI. The reliability quantifies the uncertainty in the relationship between the electrical conductance and the steam flow magnitude. We have two interpretations of the clay cap from the 3D MT inversion and one from 1D models. In order to have sufficient measurements to compute statistics, we will use all conductivity measurements separately from each clay cap used to calculate the geometric means of conductance on the x-axes of Figure 5c, Figure 7 and Figure 9. Therefore, three data reliabilities will be computed corresponding to the three clay cap calibrations (Figure 5c, Figure 7 and Figure 9). Figure 10, Figure 11, and Figure 12 depict the counts of every conductance measurement from Figure 5c, Figure 7 and Figure 9: the clay cap defined by a threshold of 0.12 S/m, 0.10 S/m and with the gridded 1D models respectively. The counts in the histograms are represented by  $c_{ij}$ , where  $c$  is the total number of measurements that fall within conductance bin  $j$  and are associated with one of the seven steam flow categories  $i$  (Equation 2).

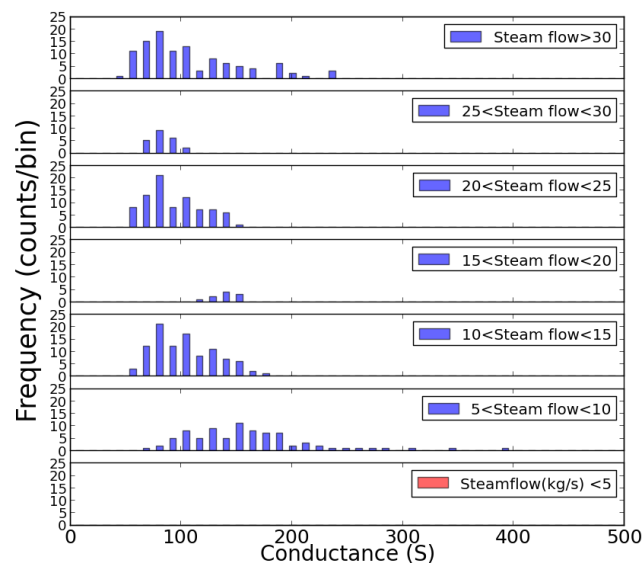


Figure 10: From clay cap defined by 0.12 S/m : counts (blue bars) of conductance measurements in bin  $j$  (horizontal axis) that correspond to steam flow bin  $i$  (different vertical rows).

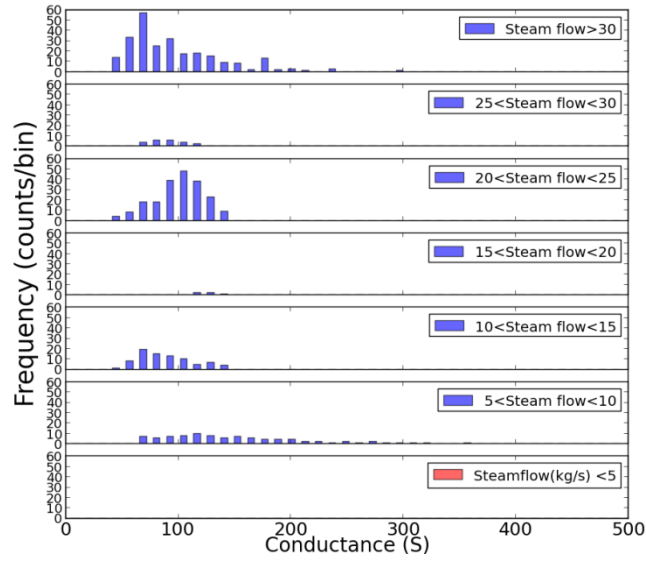


Figure 11: From clay cap defined by a) 0.10 S/m: counts (blue bars) of conductance measurements in bin  $j$  (horizontal axis) that correspond to steam flow bin  $i$  (different vertical rows).

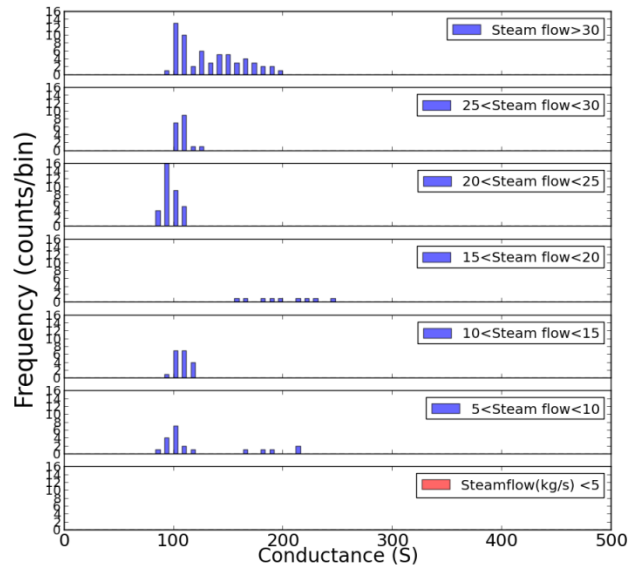


Figure 12: Counts (blue bars) of conductance measurements in bin  $j$  (horizontal axis) that correspond to steam flow bin  $i$  (different vertical rows). From clay cap defined by 1D MT models

The data likelihood (which is also the reliability) considers how likely a conductance bin is given that we know the steam flow categories ( $\theta_i$ ) associated with it. Therefore, the counts in bin  $ij$  are normalized by the total number of measurements in that steam flow category ( $i$ ):

$$Pr(G = g_j | \Theta = \theta_i) = \frac{c_{ij}}{\sum_i c_{ij}} \quad (4)$$

$$i = \{1, 2, 3, 4, 5, 6, 7\} \quad j = 1, \dots, J$$

where the electrical conductance is represented by  $g$ . The denominator,  $\sum_i c_{ij}$ , represents normalization by the sum of all data points within that steam flow category ( $\theta_i$ ). For example, in Figure 10 for  $\theta_i > 30$  and  $50S < \text{conductance} \leq 60S$ ,  $Pr(G = g_j | \Theta = \theta_i) = \frac{2}{2} = 100\%$ , because the steam flow category  $\theta_i > 30$  exclusively has measurements in this conductance bin. However, for the next conductance bin up ( $60S < \text{conductance} \leq 70S$ ), the likelihood for  $\theta_i > 30$  drops to  $Pr(G = g_j | \Theta = \theta_i) = \frac{10}{20} = 50\%$  because two other steam flow categories are associated with this conductance. Next, we want to establish the information posterior which establishes a “misinterpretation rate” or how uniquely a conductance bin can distinguish between any of the steam flow categories  $\theta_i$ . According to Bayes law, the posterior ( $Pr(\Theta = \theta_i | G = g_j)$  in Eqn. 5 below) is equal to the product of the prior probability ( $Pr(\Theta = \theta_i)$ ) and the likelihood ( $Pr(G = g_j | \Theta = \theta_i)$ ) scaled by the marginal ( $Pr(G = g_j)$ ):

$$\begin{aligned} Pr(\Theta = \theta_i | G = g_j) &= \frac{Pr(\Theta = \theta_i) Pr(G = g_j | \Theta = \theta_i)}{\sum_{k=1}^{N+1} Pr(\Theta = \theta_k) Pr(G = g_j | \Theta = \theta_k)} \quad (5) \\ &= \frac{Pr(\Theta = \theta_i) Pr(G = g_j | \Theta = \theta_i)}{Pr(G = g_j)} \quad i \\ &= \{1,2,3,4,5,6,7\} \quad j = 1, \dots, J \end{aligned}$$

The corresponding posteriors of the different counts in Figure 10, Figure 11, and Figure 12 are the solid colored lines in Figure 13, Figure 14, and Figure 15 respectively. When the posterior is close to 1 or 0 (right hand y-axis label), this indicates that the data in that conductance bin is more informative (the misinterpretation rate is lower). The posteriors in Figure 13, Figure 14, and Figure 15 were calculated using the least optimistic prior shown in Table 1 to include the possibility of encountering a low or zero steam flow. For conductance values that were not represented in each of the particular calibration data sets (e.g. where no bars exist), the posterior probability is distributed according to the prior probability across the 7 steam flow bins.

Therefore, we see that the steam flow  $\theta < 5$  category is given a high probability for conductance bins where no data was represented in the calibration data. The count bars are the same in Figure 13, Figure 14, and Figure 15 as in Figure 10, Figure 11, and Figure 12 respectively, however each is now colored from dark green to red. These will be explained in Section 3.3.

Visually, the red posterior (steam flow  $> 30$  kg/s) from the clay cap defined by the 0.12 S/m threshold (top of Figure 13s) has a high posterior ( $\sim 1$ ) value for the conductance bins at  $G=50$  S. This will contribute to a higher VOI evaluation. The posterior for  $\theta > 30$  for the 0.10Sm clay cap is similar: consistently high for conductance bins 50-90 S. However, in the integrated analysis, the conductance bins of 90-110 S (the lowest conductances) are more equally distributed between these three steam flow bins. Thus, the posterior is not high for the highest steam flow within these conductance bins (90-110 S) rather the highest posterior here is for the bins of 140-160 S, as only these conductances values were uniquely related to steam flow  $> 30$  kg/s.

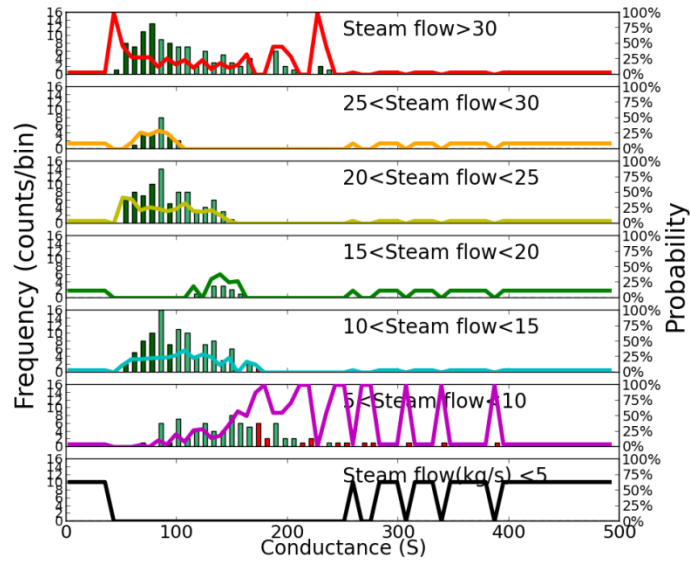


Figure 13: Counts (blue bars) and posteriors (solid lines) for the clay cap interpretations defined at 0.12 S/m. For each conductance bin, the sum of the posterior across the steam flow categories equals 100%. The colors of the conductance bars correspond to the value calculated for each conductance bin (equation 10): upper quartile is darkest green, while red is the lowest quartile.

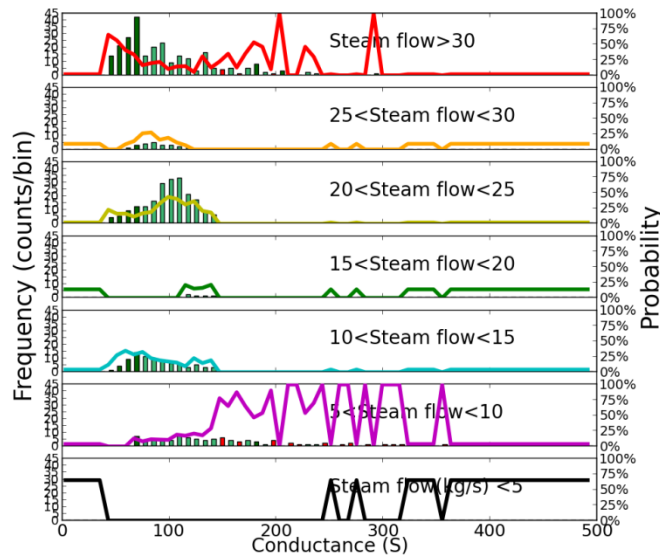


Figure 14: Counts (blue bars) and posteriors (solid lines) for clay cap interpretation defined at 0.10 S/m. For each conductance bin, the sum of the posterior across the steam flow categories equals 100%. The colors of the conductance bars correspond to the value calculated for each conductance bin (equation 10): upper quartile is darkest green, while red is the lowest quartile.

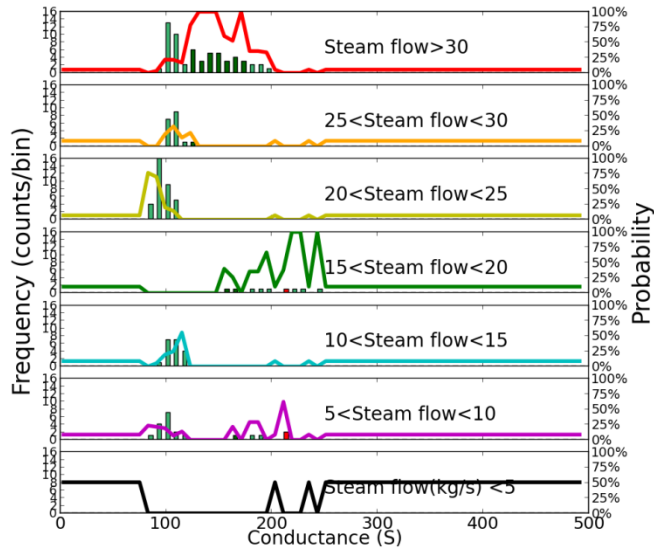


Figure 15: Counts (blue bars) and posteriors (solid lines) for the clay cap interpretation with combine 1D MT. For each conductance bin, the sum of the posterior across the steam flow categories equals 100%. The colors of the conductance bars correspond to the value calculated for each conductance bin (equation 10): upper quartile is darkest green, while red is the lowest quartile.

### 3. VOI Calculation: Description & Results

This section describes the calculations necessary to estimate the value of imperfect information using the information posteriors plotted in Figure 13. First, the  $V_{\text{prior}}$  or the prior value is described.

#### 3.1 $V_{\text{prior}}$ : the best decision option given prior uncertainty

We will now describe how each prior model is linked to possible economic outcomes. This will be summarized in the quantity  $V_{\text{prior}}$ , which translates our prior uncertainty (our current state of information) into an expected (or average) outcome from our decision.

Recall that decision analysis frames the decision as the chance to enter the geothermal lottery with perceived chances of winning a prize (e.g. drilling into a profitable reservoir). By utilizing  $V_{\text{prior}}$ , a decision-maker can logically determine when one should participate in this lottery given both the prior uncertainties and possible gains and losses. The value metric allows for comparison between outcomes from different decision alternatives, which can be represented by function  $d_a$ .

$$v_a^{(t)}(\theta_i) = d_a(\mathbf{z}(\Theta = \theta_i)^{(t)}) \quad (6)$$

$$a = 1, 2 \quad i = 1, \dots, 7 \quad t = 1, \dots, T$$

We assume only 2 possible alternatives ( $a = 1$  or  $2$ ): drill/produce the reservoir or do nothing. Table 1 defines the 14 possible outcomes, which is a result of these 2 decision alternatives and the 7 possible reservoir categories. The columns represent the decision alternatives ( $a=1$  and  $a=2$ ) and the rows the different steam flow categories ( $\theta_i$ ).

**Table 2: Table of nominal value outcomes for the 2 possible decision options (columns) and 7 possible economic viability categories of the unknown subsurface (rows).**

Decision option→ ↓Steam Flow Rate (kg/s)	$v_{a=1}^{(t)}(\theta_i)$ a = 1 (drill under cap)	$v_{a=2}^{(t)}(\theta_i)$ a = 2 (do nothing)
$\theta_i > 30$	\$700,000	\$0
$25 \leq \theta_i \leq 30$	\$300,000	\$0
$20 \leq \theta_i \leq 25$	\$125,00	\$0
$15 \leq \theta_i \leq 20$	\$40,000	\$0
$10 \leq \theta_i \leq 15$	\$0	\$0
$5 \leq \theta_i \leq 10$	-\$200,000	\$0
$\theta_i \leq 5$	-\$500,000	\$0

Table 2 represents hypothetical, monetary values that could represent relative gains (payouts-- shown in black-- when you drill a well with economic production rates) or losses (loss on investment --shown in red--when you drill an uneconomic well). Specific (and more realistic) gains and losses for a particular field site can be easily substituted in Table 1 and into the methodology. This would be necessary to use the resulting VOI's to determine if a particular data type is worth purchasing at a specific field site. The values in Table 1 are simply for demonstration purposes so that the behavior of the VOI quantities can be visualized.

All the necessary quantities have been introduced to calculate  $V_{prior}$ .

$$V_{prior} = \max_a \left( \sum_{i=1}^7 Pr(\Theta = \theta_i) v_a(\theta_i) \right) \quad (7)$$

$a = 1, 2$

In words,  $V_{prior}$  quantifies the best the decision-makers can do with the current uncertainty (no MT data has been collected), which are reflected in the prior probabilities  $Pr(\Theta = \theta_i)$ .  $V_{prior}$  identifies which decision alternative gives *on average* the best outcome (done through the  $\max_a$ ).

When considering a specific location for geothermal exploration, these prior probabilities should come from a geologist and/or other experts with knowledge of the geologic structure and history. For our base case (column  $a$  of Table 2), we assume  $Pr(\Theta = \theta_1) = 40\%$  (steam flow < 5 kg/s) and all other categories  $Pr(\Theta = \theta_i) = 10\%$   $i = 2, \dots, 7$ . Two other prior probabilities are included to demonstrate the influence of the prior on the final VOI: both reflecting an increase in optimism that the highest steam flow category has greater chance of occurring. The column b) of Table 2 is the Intermediate prior, where the probability of the lowest steam flow class has dropped to 20% from 40% and the greatest steam flow class is now 13%, up from 10%. The most optimistic prior (column c) reverses the probabilities for the greatest and smallest steam flow bins from the base case.

**Table 3: Table of 3 possible prior probabilities (columns) for the 7 possible economic viability categories of the unknown subsurface (rows), additionally the resulting  $V_{prior}$ ,  $V_{perfect}$  and  $VOI_{perfect}$  for these priors ( $V_{perfect}$  and  $VOI_{perfect}$  will be explained in 3.2).**

Prior Uncertainty→ ↓Steam Flow Rate (kg/s)	a) Least optimistic $Pr(\Theta = \theta_i)$	b) Intermediate $Pr(\Theta = \theta_i)$	c) Most optimistic $Pr(\Theta = \theta_i)$
--	---	---	--

$30 \leq \theta_i$	10%	13%	40%
$25 \leq \theta_i \leq 30$	10%	13%	10%
$20 \leq \theta_i \leq 25$	10%	13%	10%
$15 \leq \theta_i \leq 20$	10%	13%	10%
$10 \leq \theta_i \leq 15$	10%	13%	10%
$5 \leq \theta_i \leq 10$	10%	15%	10%
$\theta_i \leq 5$	40%	20%	10%
$V_{prior}$	\$0	\$21,450	\$256,500
$V_{perfect}$	\$116,500	\$151,450	\$326,500
$VOI_{perfect}$	\$116,500	\$130,000	\$70,000

Returning to the lottery example, when  $V_{prior}$  is 0, the decision-maker should “not participate in the lottery” (i.e. don’t drill) given the current state of information.  $V_{prior}=0$  tells the decision-maker that the decision alternative to “do nothing” will yield the higher outcome on average.  $V_{prior}=0$  reflects the potential for large losses when you “participate in the lottery” or drill to produce a geothermal reservoir. The decision-maker would only be wise to participate in the lottery when  $V_{prior} > 0$ . The three different  $V_{prior}$ ’s for each of the prior probabilities are shown in Table 3, which use the value outcomes of Table 2. For the base case prior probabilities (the least optimistic),  $V_{prior} = \$0$ .  $V_{prior}$  increases to \$21,450 and \$256,500 for the intermediate and most optimistic priors. Intuitively this makes sense since both priors reflect higher probabilities for higher-valued outcomes.

### 3.2 $VOI_{perfect}$ : Upper bound on the value of information

The value of perfect information can be calculated using Equation 1, by substituting in  $V_{perfect}$  for the value with information ( $V_{with\ information}$ ).  $VOI_{perfect}$  assumes that an information source exists that will always identify the correct economic viability category  $\theta_i$  without errors. Like  $V_{prior}$ ,  $V_{perfect}$  only depends on the prior uncertainty and potential gains/losses of the problem.

$$V_{perfect} = \sum_{i=1}^7 Pr(\Theta = \theta_i) \left( \max_a v_a(\theta_i) \right) \quad (8)$$

Here, we see that for each steam flow rate category  $\theta_i$ , we can choose the best decision alternative  $a$  (this is reflected in  $\max$  being calculated before the weighted average). With perfect information, we always know when the reservoir is uneconomic, and therefore we will always choose not to participate in the lottery. Thus, we remove the chance of loss by collecting perfect information. With our current state of information, we would not enter the lottery when the potential losses were too high relative to the gains. But with a flawless information source to allow us to avoid these losses, we may choose to participate in the lottery. Since it assumes error-free information, the  $VOI_{perfect}$  quantity will give an upper bound on what we could expect for any information source. For the base case example, using the values in Table 1,  $V_{perfect} = \$116,500$ . Following Equation 1

$$VOI_{perfect} = V_{perfect} - V_{prior} \quad (9)$$

Thus, since  $V_{prior} = \$0$ ,  $VOI_{perfect} = \$116,500$ .

### 3.3 $VOI_{imperfect}$ Results: Different Clay Cap Interpretations

Now we consider imperfect MT data and we estimate its reliability when distinguishing between the seven different possible steam flow categories  $\theta_i$ . The data is from a specific location, and we are using it to generate the required information posterior ( $Pr(\Theta = \theta_i | G = g_j)$ ), which influences  $VOI$ , but everything else (priors, value outcomes, etc.) is completely unrelated to the location and settings of the actual data set. The information posterior ( $Pr(\Theta = \theta_i | G = g_j)$ ) is the form actually used to calculate the value *with* imperfect information  $V_{imperfect}$ .

$$V_{imperfect} = \sum_{j=1}^J Pr(G = g_j) \left\{ \max_a \left[ \sum_{i=1}^7 Pr(\Theta = \theta_i | G = g_j) v_a(\theta_i) \right] \right\} \quad (10)$$

Here, the posterior accounts for how often one may incorrectly infer a steam flow category given the inverted electrical conductance. The posterior is used to weigh the averaged outcome of each alternative and category combination  $v_a(\theta_i)$ . Since the decision is made after conductivity data has been collected, the best alternative (max) is chosen given the interpreted category. Lastly,

$V_{imperfect}$  is weighted by the marginal probability  $Pr(G = g_j)$ , how often any of the particular inverted resistivities occur relative to other conductivity bins.

Table 3: Table of **nominal**  $V_{imperfect}$  and  $VOI_{imperfect}$  for the 3 clay cap interpretations (columns) for 3 different priors.

Prior Probability:	Clay Cap defined by threshold:	0.12 Siemens/m	0.10 Siemens/m	Integrated interpretation from MT, methylene blue, temperature
Least optimistic (base case)	$V_{imperfect}$	\$100,800	\$100,500	\$97,500
	$VOI_{imperfect}$	\$100,800	\$100,500	\$97,500
Intermediate	$V_{imperfect}$	\$128,000	\$127,800	\$122,700
	$VOI_{imperfect}$	\$106,500	\$106,300	\$101,200
Most optimistic	$V_{imperfect}$	\$310,800	\$309,300	\$307,200
	$VOI_{imperfect}$	\$54,300	\$52,800	\$50,700

Table 3 includes both the value with imperfect information ( $V_{imperfect}$ ) and the value of imperfect information ( $VOI_{imperfect}$ ). The value of imperfect information ( $VOI_{imperfect}$ ) is calculated using Equation 1 where now the  $V_{imperfect}$  is used in place of the generic term of  $V_{with\ information}$ .

$$VOI_{imperfect} = V_{imperfect} - V_{prior} \quad (11)$$

As expected, all the  $VOI_{imperfect}$ 's estimates are lower than their respective  $VOI_{perfect}$ 's (\$116,500, \$130,000, \$70,000). This demonstrates how the highest value outcome will not be realized because of the imperfectness of the data that can mislead the decision maker about the economic viability of the reservoir. **The three  $VOI_{imperfect}$  results are not significantly different from each other for any of the prior probability cases.** The  $VOI_{imperfect}$  assessed from the clay cap defined at 0.12S/m is slightly higher for all three cases which can be explained by the posterior being ~1 for the highest steam flow category (Figure 13).

### 3.4 VOI for determining the next location to drill

The next set of results demonstrates how the information posteriors ( $Pr(\Theta = \theta_i | G = g_j)$ ) and the decision outcomes (Table 1) can be used to determine new locations for drilling that may have higher likelihood of success. Essentially, each conductance bin ( $j$ ) can be assigned a value which is calculated in the inner two evaluations of Equation 9

$$v_j = \left\{ \max_a \left[ \sum_{i=1}^7 Pr(\Theta = \theta_i | G = g_j) v_a(\theta_i) \right] \right\} \quad (11)$$

The first evaluation is a weighted average of possible outcomes ( $v_a(\theta_i)$ ) using the posterior as the weights. The next operation is the non-linear max, which identifies the best alternative given the misinterpretations possible for that conductance bin. The color of the bins (dark green, green, light green and red) in Figure 13, Figure 14, and Figure 15 reflect the four quartiles of  $v_j$  for each conductance bin  $j$ . Therefore, in the case where the posterior nearly definitively identifies the highest steam flow category (as in the case of Figure 13, steam flow  $> 30$ ), the  $v_j$  will be highest. But if no conductance range (bin) exists that exclusively (or close to exclusively) can identify the higher steam flow category, the  $v_j$ 's will reflect this. This is seen in Figure 13 for conductance of  $\sim 175$  S, where the bars are red. In short,  $v_j$  depends on both the posterior and the value attached to steam flow category most related to that conductance bin.

For this particular field, a future drilling campaign is considered in an area covered by the current MT inversion, but no drilling has taken place and therefore, no existing steam flow information is available. We can plot the  $v_j$ 's according to the MT inversion model and look specifically at the area under consideration for future drilling. This may guide future well locations by using the past performance of MT to locate high steam flow.

However, the conductance's represented in the current MT inversion, may not be included in the calibrated data set. For example, there are no conductance's  $< 50$  S that were "collocated" to a steam flow datum (Figure 10, Figure 11, and Figure 12), but the conductance maps of the different clay cap interpretations (shown in Figure 16, Figure 17, and Figure 18) have large areas with conductance's  $< 50$  S (shown in dark and light purples). Therefore, the posterior for these values are distributed according to the assigned prior probabilities as described in Section 2.3. Thus conductance's  $< 50$  S have  $v_j$ 's in the lowest quartile, since they are tied to the steam flow  $< 5$  kg/s. This interpretation could be changed, but since these conductance's were not related to any production data, this could be considered a conservative approach.

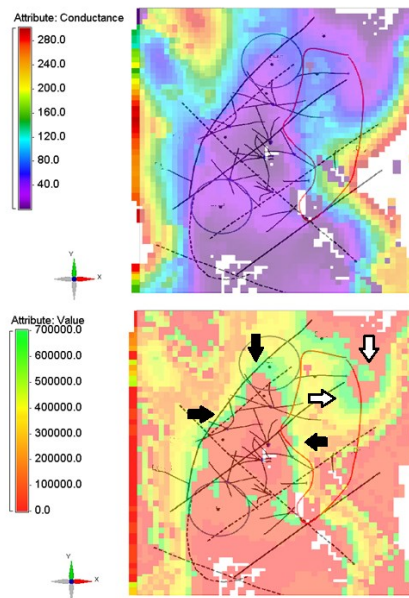


Figure 16: Plane View of field. Area within red solid line and the two black circles denotes location of possible future drilling campaign. a) conductance of clay cap interpreted with 0.12 S/m threshold b) value (4) for each conductance bin ( $v_j$ ) calculated using posterior in Figure 13.

Figure 16a displays the conductance (S) of the clay cap and Figure 16b displays the corresponding values in dollars (Equation 10) for the clay cap interpreted only with a 0.12S/m threshold. Overlain is the map of the field with surface traces of the faults (dashed black) and the area under consideration for future drilling (red solid line). Thus, by mapping back the value of each conductance bin,  $v_j$ 's provides some spatial guidance on where drilling future development wells may produce a high valued result, given the relationship of current production with the interpreted MT data. Figure 17 and Figure 18 contain the conductance and value for the clay caps interpreted by the 0.10 S/m threshold and the integrated analysis respectively. Figure 16 and Figure 17 display very similar value patterns which makes sense since they differ by only a small conductivity cut-off. They display higher value outcomes around the northeast and northwest margins of the resource (the black arrows point to this feature) that follows the arching fault on the western boundary of the field. They also both have another northwest-southeast green (high value) feature intersecting the northern section of the red circle (white arrows). Recall, that the value is a function of *both* the conductance bin's ability to exclusively identify a steam flow category ( $\theta$ ) and how economic that category is. Generally for these two calibrations, conductance bins  $<100\text{S}$  but  $>50\text{ S}$  had the strongest relationship with the highest steam flow.

However, the integrated analysis, Figure 18, shows a green feature that is slightly shifted north (black arrows) of what is shown in Figure 16 and Figure 17. Additionally, the integrated analysis demonstrates there is more promise (green) in the central section of the exploration area than the two threshold calibration methods (white arrows). This is a direct result of how the conductance bins  $\sim 180\text{-}210\text{S}$  had the most exclusive relationship with the highest steam flow category ( $\theta > 30\text{ kg/s}$ ). Therefore, there green features of Figure 18 correlate with this range of conductance bins.

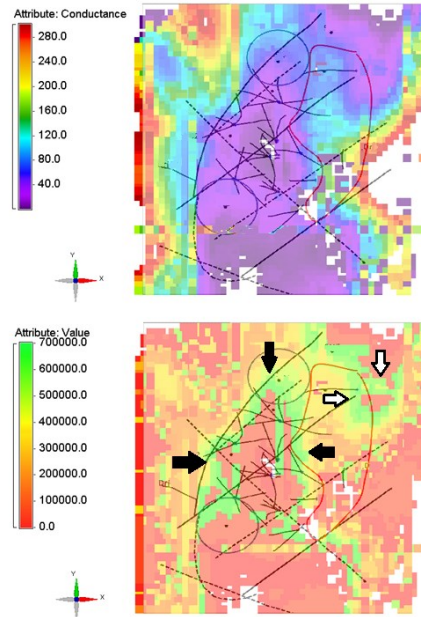


Figure 17: Plane View of field. Area within red solid line denotes location of possible future drilling campaign. a) conductance of clay cap interpreted with a 0.10 S/m threshold. b) value for each conductance bin ( $v_j$ ) calculated using posterior in Figure 14.

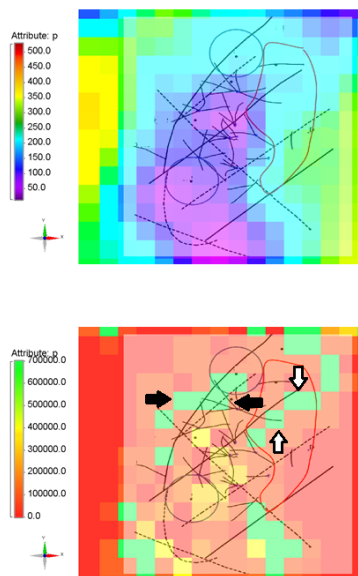


Figure 18: Plane View of clay cap interpreted with integrated analysis. Area within red solid line denotes location of possible future drilling campaign. a) conductance calculated from MT inversion model b) value for each conductance bin ( $v_j$ ) calculated using posterior in Figure 15.

## 4. Conclusions

VOI is used to determine whether a particular type of data is worth acquiring and thus, the VOI must be calculated before the intended data is collected. We use a calibrated data set (electrical conductivity model from MT collocated with steam flow measurements) to estimate the past

performance of MT to delineate the boundaries of the clay cap. Therefore, we assume that this VOI will be used to decide whether or not to purchase MT data at analog field sites in the future. Specifically, we estimated the reliability of the data to reveal the principal uncertainty to the decision ( $\theta_i$  representing steam flow for our example). In turn, we described how the value of imperfect information could be calculated given this reliability. We use a hypothetical decision scenario of “to drill or not” to define the other drivers of VOI: the prior probability, the value outcomes of Table 1. These would need to be refined in order to use these VOI estimates to determine whether or not to purchase the information.

This study indicates that the different interpretations of the clay cap do not greatly impact the assessed VOI of the MT data. From a decision analysis stand point, the different  $VOI_{\text{imperfect}}$ 's are indistinguishable since they are within \$4,000 of each other, and therefore, the decision to purchase MT or not would be the same given the result of these three  $VOI_{\text{imperfect}}$ 's

We also used VOI to aid in determining future drilling locations. These relied on the information posteriors calculated for each clay cap interpretation and the value outcomes of Table 1. All three demonstrated consistent patterns with the known fault traces. As expected, the value maps for the two calibrations that only relied on electrical conductivity thresholds were quite similar. The value map (Figure 18b) that used temperature, electrical conductivity and methylene blue data had slightly different “green” (higher potential drill sites) features than the other two (Figure 16b and Figure 17b). The three value maps can be used by the operators and local experts to provide information on how they may prioritize and target their next well(s).

We appreciate funding from the DOE Geothermal Technologies Office. This research was performed under the auspices of the U.S. Department of Energy by Lawrence Livermore National Laboratory under Contract No. DE-AC52-07NA27344. LLNL-CONF-649076.

## References

- Bratvold, R. B., Bickel, J. E., Risk, A., & Lohne, H. P. (2009). Value of Information in the Oil and Gas Industry : Past, Present, and Future. *Society of Petroleum Engineers: Reservoir Evaluation & Engineering*, (August 2009), 11–14. doi:10.2118/110378-PA
- Cumming, W. (2009). Geothermal resource conceptual models using surface exploration data. In *PROCEEDINGS, Thirty-Fourth Workshop on Geothermal Reservoir Engineering* (p. SGP-TR-187). Stanford, California.
- Gunderson, R., Cumming, W., Astra, D., & Harvey, C. (2000). Analysis of smectite clays in geothermal drill cuttings by the methylene blue method : for well site geothermometry and resistivity sounding correlation. In *Proceedings World Geothermal Congress* (pp. 1175–1181).
- Karlsdóttir, R., Vilhjálmsson, A., Árnason, K., & Beyene, A. (2012). *Þeistareykir Geothermal Area , Northern Iceland 3D Inversion of MT and TEM Data* (p. 173). Reykjavík. Retrieved from www.isor.is
- Newman, G. A., & Alumbaugh, D. L. (2000). Three-dimensional magnetotelluric inversion using non-linear conjugate gradients. *Geophysical Journal International*, 140(2), 410–424. doi:10.1046/j.1365-246x.2000.00007.x
- Pratt, J., Raiffa, H., and Schlaifer, R. (1995). *Introduction To Statistical Decision Theory*. Cambridge, MA: The Massachusetts Institute of Technology Press.
- Rejeki, S., Rohrs, D., Nordquist, G., & Fitriyanto, A. (2010). Geologic Conceptual Model Update of the Darajat Geothermal Field , Indonesia. In *Proceedings World Geothermal Congress 2010* (pp. 25–29).

Trainor-Guitton, W. J., Hoversten, G. M., Ramirez, A., Roberts, J., Juliusson, E., Key, K., & Mellors, R. (2014). The value of spatial information for determining well placement: A geothermal example. *Geophysics*, 79(5), W27–W41. doi:10.1190/geo2013-0337.1

Trainor-Guitton, W. J., Ramirez, A., Ziagos, J., Mellors, R., & Roberts, J. (2013). An Initial Value Of Information ( VOI ) Framework For Geophysical Data Applied To The Exploration Of Geothermal Energy. In *PROCEEDINGS, Thirty-Eighth Workshop on Geothermal Reservoir Engineering, Stanford University, Stanford, California, February 11-13, 2013 SGP-TR-198*.

Trainor-Guitton, W. J., Ramirez, A., Ziagos, J., Mellors, R., Roberts, J., Juliusson, E., & Hoversten, G. M. (2013). Value of Spatial Information for Determining Geothermal Well Placement. *Geothermal Resources Council Transactions*, 1–18.

Ussher, G., Harvey, C., Johnstone, R., Anderson, E., & Zealand, N. (2000). Understanding the resistivities observed in geothermal systems. In *Proceedings World Geothermal Congress* (pp. 1915–1920).

## *Appendix B*

---

### *Additional publications (as separate documents)*

---

Trainor-Guitton, W. J., G. M. Hoversten, A. Ramirez, J. Roberts, E. Juliusson, K. Key, and R. Mellors, 2014a, The value of spatial information of for determining well placement: a geothermal example, *GEOPHYSICS* 79, 5(2014); pp. W27-W41 (15 pages)  
<http://dx.doi.org/10.1190/geo2013-0337.1>, Online Publication Date: 25 Aug 2014

Trainor-Guitton, W., M. Hoversten, E. Juliusson, A. Ramirez, J. Roberts, and R. Mellors, 2014b, Value of Information Assessment using Calibrated Geothermal Field Data, Proceedings of the 39th Stanford Geothermal Workshop, Feb. 24-26, 2014, Stanford, CA.